

# Active and passive viscosities of a bent-core nematic liquid crystal

S. Dhara,<sup>1,\*</sup> Y. Balaji,<sup>1</sup> J. Ananthaiah,<sup>1</sup> P. Sathyanarayana,<sup>1</sup> V. Ashoka,<sup>1</sup> A. Spadlo,<sup>2</sup> and R. Dabrowski<sup>2</sup>

<sup>1</sup>*School of Physics, University of Hyderabad, Hyderabad 500046, India*

<sup>2</sup>*Institute of Chemistry, Military University of Technology, 00-908 Warsaw, Poland*

(Received 4 February 2013; published 29 March 2013)

We report the measurements of active and passive viscosities of a bent-core nematic liquid crystal. The active viscosity is measured using a rheometer and the passive viscosities are measured by measuring the self-diffusion coefficient of a microsphere in the aligned sample. The effective active viscosity is larger and the effect of presmectic fluctuations are observed much higher than the  $N$ -Sm-C transition temperature than commonly seen in calamitic liquid crystals. The temperature dependence of passive viscosities is stronger than that of active viscosities. The self-diffusion of the microsphere is reduced and appears to be non-Gaussian as the  $N$ -Sm-C transition is approached. The study of Brownian fluctuations is useful to understand the smectic fluctuations in bent-core nematic liquid crystals.

DOI: [10.1103/PhysRevE.87.030501](https://doi.org/10.1103/PhysRevE.87.030501)

PACS number(s): 64.70.mj, 83.80.Xz, 66.20.Ej

The viscosity of liquid crystals strongly depends on the microscopic structure of the constituent molecules and the mesophases. There are several theoretical and experimental studies of the low molecular weight liquid crystals where the molecules have mostly cylindrical symmetry [1–3]. It is known that the nematic  $N$  phase has three principal viscosities called Miesowicz viscosities, namely,  $\eta_1$ ,  $\eta_2$ , and  $\eta_3$ , depending on the direction of the shear and the orientation of the liquid crystal director (the average alignment direction of the long axes of the molecules). A schematic representation of the director orientation in a calamitic (rodlike) nematic liquid crystal with respect to the shear and corresponding viscosities is shown in Fig. 1. These viscosities can be expressed in terms of Leslie coefficients  $\alpha_1$ – $\alpha_6$ , which are used to define the nematic stress tensor. In nematic liquid crystals, both  $\alpha_2$  and  $\alpha_3$  are negative close to the nematic-isotropic ( $N$ - $I$ ) transition and the director is aligned along the flow direction with an angle  $\theta = \tan^{-1}(\sqrt{\alpha_2/\alpha_3})$  [4,5]. However, if the compounds also have a smectic- $A$  (Sm- $A$ ) phase below the  $N$  phase,  $\alpha_3$  is renormalized (i.e.,  $\alpha_3^R > 0$ ) a few degrees below the  $N$ - $I$  transition temperature. As a result, the ratio  $\alpha_2/\alpha_3$  becomes negative and the director changes its orientation to the neutral direction ( $x$  axis). As the temperature is further reduced it has been shown theoretically that  $\dot{\gamma}\tau \rightarrow 1$ , where  $\dot{\gamma}$  and  $\tau$  are the shear rate and relaxation time of the critical fluctuations and consequently  $\alpha_3^R$  tend to diverge a few degrees above the  $N$ -Sm- $A$  transition [6]. As a result, the director undergoes precessional motion with an angular frequency  $\omega_0$  along the neutral direction that can be described by the equation of an ellipse  $n_y^2(t)/n_{y0}^2 + n_z^2(t)/n_{z0}^2 = 1$ , where  $n_y(t) = n_{y0}\cos(\omega_0 t)$  and  $n_z(t) = n_{z0}\sin(\omega_0 t)$  are components of the director  $\mathbf{n}(t) = [n_x(t), n_y(t), n_z(t)]$ . Several steady state structures are observed experimentally [6], depending on the relative strength of the director components, and are denoted by  $a_m$  ( $n_{y0} > n_{z0}$ ),  $a_s$  ( $n_{y0} = n_{z0}$ ),  $a(b)$  ( $n_{y0} < n_{z0}$ ), and  $a_c$  ( $n_{y0} \ll n_{z0}$ ). The above structural features are also reflected in the static dielectric measurements on a few calamitic compounds exhibiting a  $N$ -Sm- $A$  phase transition [7,8]. Liquid crystals of bent-core

molecules have created immense interests [9,10]. Usually these molecules have a strong tendency to form smectic phases. However, they occasionally exhibit a nematic phase in which the physical properties are reported to be significantly different from conventional calamitic nematic liquid crystals [11–19]. The presence of temporarily fluctuating smectic clusters is also evident in many experiments. In this context the measurement of flow or shear viscosity in the bent-core liquid crystals is very rare. The major problem in such measurements is the requirement of a large sample, which in general is not easy to get. In the present paper we report on the measurement of active and passive viscosities of a bent-core liquid crystal. We show that the temperature-dependent behaviors of the active and passive viscosities are noticeably different and the study of self-diffusion of a microsphere is a sensitive technique to investigate the presmectic fluctuations in bent-core nematic liquid crystals.

The chemical structure and the phase transition temperatures of the bent-core nematic (BCN) are shown in Fig. 2(a), which exhibits the following phase transitions (cooling):  $I$  at 176.4 °C to  $N$  at 118.3 °C to Sm- $C$  at 101.3 °C to Sm- $X$  at 90.4 °C to Sm- $Y$  at 60.2 °C in Cr. The purity of the compound was confirmed by high-performance chromatography and other techniques. The active viscosity measurements were made using a rheometer (Anton Paar MCR 501) in plate-cone geometry with a plate diameter of 50 mm and a cone angle of 1°. The plates were not treated for any specific orientation of the molecules. The temperature of the sample was controlled with a Peltier temperature controller within an accuracy of 0.1 °C. We used a videomicroscopy technique to measure the self-diffusion coefficients of a tiny silica microsphere (with a diameter of 0.98  $\mu\text{m}$ ) and hence the passive viscosities of the sample parallel and perpendicular to the director. To promote a specific molecular alignment on the surface the silica microspheres were coated with octadecyldimethyl (3-trimethoxysilylpropyl) ammonium chloride (DMOAP) before mixing with the liquid crystal [20]. The Brownian fluctuations of an isolated microsphere in a planar cell ( $d = 23 \mu\text{m}$ ) was recorded and the position was determined with the help of an appropriate computer program. The histogram of the microsphere displacements were fitted to Gaussian with a probability  $P$  that the particle would diffuse a certain distance

\*Corresponding author: [sdsp@uohyd.ernet.in](mailto:sdsp@uohyd.ernet.in)

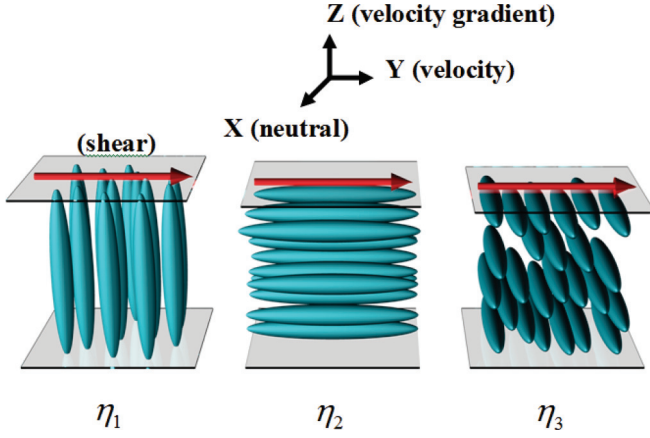


FIG. 1. (Color online) Schematic representation of the three fundamental director orientations in the nematic phase with respect to the direction of shear. Miesowicz viscosities corresponding to each orientation are designated by  $\eta_3$ ,  $\eta_2$ , and  $\eta_1$ , respectively.

$\delta$  in the time interval  $\tau$  is  $P(\delta|\tau) = P_0(\tau)\exp(-\delta^2/\Delta^2(\tau))$ , where  $\Delta(\tau)$  is the width of the distribution and  $P_0(\tau)$  is the normalization constant. The self-diffusion coefficients of the microsphere parallel ( $D_{||}$ ) and perpendicular ( $D_{\perp}$ ) to the director are obtained by using the relation  $D_{||,\perp} = \Delta_{||,\perp}^2/4\tau$ . The corresponding viscosities are estimated by using the Stokes-Einstein relation  $\eta_{||,\perp} = k_B T/6\pi r D_{||,\perp}$ , where  $r$  is the radius of the microsphere [20].

We show the variation of shear stress with shear rate in Fig. 2(b) at various temperatures in the nematic phase. The sample was mounted on the rheometer in the nematic phase at a temperature of 140 °C. It is observed that the shear stress is proportional to the shear rate except in a low shear rate range ( $\dot{\gamma} \leq 2 \text{ s}^{-1}$ ) where the stress is constant,

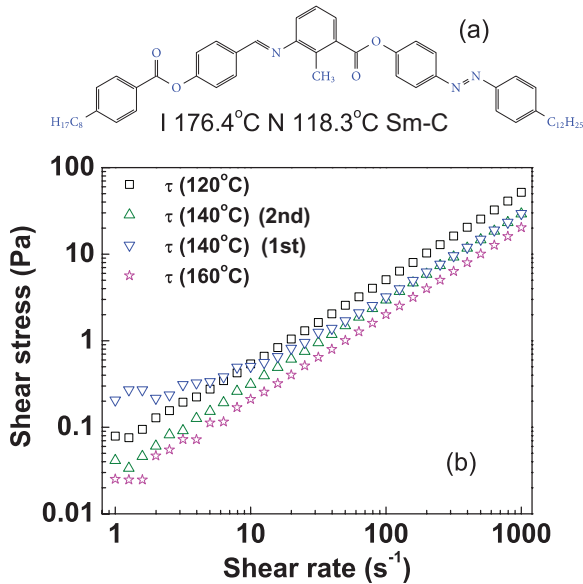


FIG. 2. (Color online) (a) Chemical structure and the first two phase transition temperatures of the bent-core compound. (b) Variation of shear stress with shear rate at various temperatures. The sample was mounted at 140 °C. Here 1st and 2nd indicate the two consecutive measurements at the same temperature.

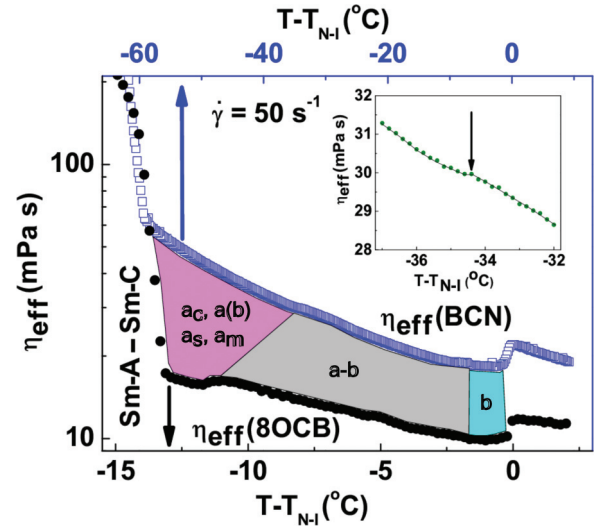


FIG. 3. (Color online) Temperature variation of  $\eta_{\text{eff}}$  in both 8OCB and BCN compounds at a shear rate  $\dot{\gamma} = 50 \text{ s}^{-1}$ . Upper and lower  $x$  axes correspond to the temperature scale of the BCN (open squares) and 8OCB (solid circles) samples, respectively. Common features indicating various steady state structures as described in the text are indicated in the shaded regions. The notation used in the shaded regions follows the notation that was used in Ref. [6] to describe the different dynamical response regimes of 8CB. In the inset, the arrow indicates a small slope change in the viscosity data of the BCN liquid crystal.

suggesting a shear thinning behavior. This could be due to the shear-induced realignment of the nematic director within the domains that are separated by disclination lines [21]. This effect is more prominent in the first measurement [140 °C (1st)], i.e., immediately after mounting the sample. Beyond  $\dot{\gamma} \simeq 2 \text{ s}^{-1}$ , the shear stress is proportional to the shear rate, hence the BCN shows the behavior of a Newtonian fluid within the experimental limit ( $\dot{\gamma} = 1000 \text{ s}^{-1}$ ). The shear-dependent viscosity of a bent-core nematic was also studied using a nanoliter rheometer by Bailey *et al.* [22] in the shear rate range of 500–10 000  $\text{s}^{-1}$ . They reported Newtonian behavior in the lower shear rate range ( $\leq 2000 \text{ s}^{-1}$ ) and non-Newtonian behavior at higher shear rates. Thus our results are consistent with their data in the lower range of the shear rates. In Fig. 3(a) we show the variation of the effective viscosity  $\eta_{\text{eff}}$  with shifted temperature (i.e.,  $T - T_{N-I}$ ) at a shear rate  $\dot{\gamma} = 50 \text{ s}^{-1}$ . The value of  $T_{N-I}$  was determined from the temperature-dependent measurement of the viscosity. Here the effective viscosity means the bulk viscosity measured in the cone-plate arrangement. We notice that  $\eta_{\text{eff}}$  is reduced below the  $N-I$  phase transition and increases with decreasing temperature. At  $T - T_{N-I} = -58^\circ\text{C}$ , it sharply changes slope and increases very rapidly, indicating a  $N$  to  $\text{Sm-C}$  phase transition. For the purpose of comparison we also measured  $\eta_{\text{eff}}$  for the 4'-octyloxy-4-cyanobiphenyl (8OCB) sample and present the results in Fig. 3. The behavior of  $\eta_{\text{eff}}$  has some common features in both compounds. It is reduced below the  $N-I$  transition, increases with decreasing temperature, and diverges at the  $N$  to  $\text{Sm-A-Sm-C}$  transition. In addition there is a small slope change in the viscosity data near the  $N$  to  $\text{Sm-A-Sm-C}$  transition in both samples. The data in the case

of the BCN are shown in the inset of Fig. 3 for clarity. In contrast, the  $\eta_{\text{eff}}$  behavior has at least two uncommon and distinct features. First,  $\eta_{\text{eff}}$  in the BCN is significantly larger than in 8OCB. For example, at  $T - T_{N-I} = -2^\circ\text{C}$ ,  $\eta_{\text{eff}}^{\text{8OCB}} = 10.2 \text{ mPa s}$  and  $\eta_{\text{eff}}^{\text{BCN}} = 18.7 \text{ mPa s}$  for 8OCB and BCN liquid crystals, respectively. Assuming we are essentially measuring  $\eta_2$  (since this temperature is close to  $N-I$ ), we assert that this viscosity is almost twice as high in the BCN than in the 8OCB liquid crystal. Second, the small slope change in  $\eta_{\text{eff}}$  of the BCN (Fig. 3) appears at a much higher temperature than that in the 8OCB liquid crystal. For example, it appears at  $24.5^\circ\text{C}$  and  $2^\circ\text{C}$  above the  $N$  to  $\text{Sm-A-Sm-C}$  phase transition for the BCN and 8OCB samples, respectively. A similar slope change in the viscosity data of 4'-octyl-4- cyanobiphenyl (8CB) in conjugation with x-ray [6] and rheodielectric data [23] was identified as the onset of precessional motion of the director at which  $\dot{\gamma}\tau \rightarrow 1$  and several steady state structures appear as discussed in the previous section. Considering the similarity to the previously measured viscosity data of 8CB and 8OCB, we conjecture that the precessional motion of the director in the present BCN sample begins far away, i.e.,  $24.5^\circ\text{C}$  above the  $N\text{-Sm-C}$  transition. Previously, some studies involving x-ray measurements indicated that this compound exhibits a uniaxial to biaxial nematic transition around  $T - T_{N-I} \simeq -30^\circ\text{C}$  [24,25]. However, concurrently various experiments indicated that this is due to the onset of smectic fluctuations and no phase biaxiality was observed [26,27]. Moreover, recently, in the same compound around a similar temperature we observed that the bend elastic constant as well as the rotational viscosity starts to increase more rapidly with the temperature [18,28]. We believe that this small slope change (Fig. 3, inset) indicates the temperature at which  $\dot{\gamma}\tau \rightarrow 1$ .

The study of Brownian fluctuations helps us understand the effect of smectic fluctuations on the passive viscosity of BCNs. The histograms of the particle displacement  $\delta|\mathbf{r}(t + \tau) - \mathbf{r}(t)|$  in both  $x$  ( $\parallel \mathbf{n}$ ) and  $y$  ( $\perp \mathbf{n}$ ) are shown in Fig. 4. It is evident that  $\Delta_{\parallel} > \Delta_{\perp}$ , implying  $D_{\parallel} > D_{\perp}$ , as expected. The ratio  $D_{\parallel}/D_{\perp}$  varies with temperature and changes from 1.4 to 1.7, which is close to the number (1.6) reported in calamitic liquid

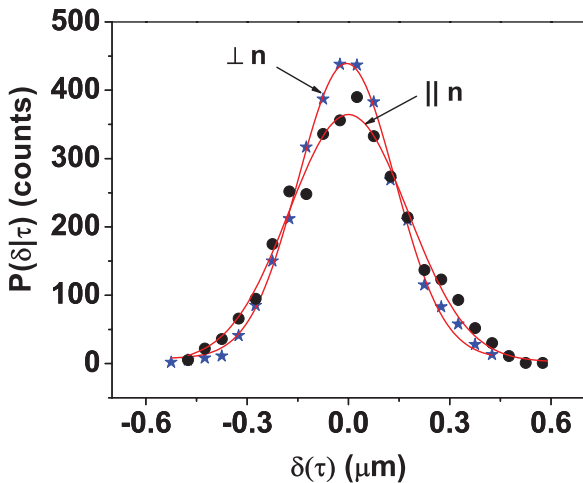


FIG. 4. (Color online) Histogram of particle displacements parallel (circles) and perpendicular (stars) to the director for  $\tau = 1 \text{ s}$ . The solid lines are Gaussian fits.

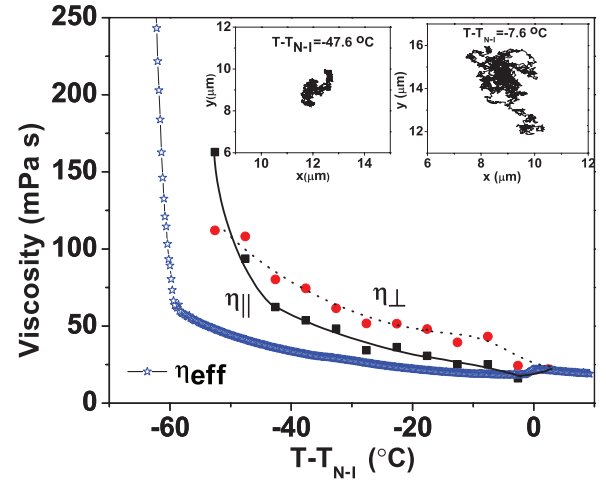


FIG. 5. (Color online) (a) Variation of  $\eta_{\text{eff}}$  (stars),  $\eta_{\parallel}$  (squares), and  $\eta_{\perp}$  (circles) as a function of shifted temperature. The inset shows the two-dimensional projection of trajectories of a microsphere closer to the  $N-I$  transition ( $T - T_{N-I} = -7.6^\circ\text{C}$ ) and closer to the  $N\text{-Sm-C}$  transition ( $T - T_{N-I} = -47.6^\circ\text{C}$ ).

crystal, e.g. 4'-pentyl-4- cyanobiphenyl with dipole defects [29]. In Fig. 5 we show the temperature variation of  $\eta_{\parallel}$  and  $\eta_{\perp}$  of the BCN liquid crystal as determined from  $D_{\parallel}$  and  $D_{\perp}$  using the Stokes-Einstein relation. We note that in the isotropic phase  $\eta_{\parallel} = \eta_{\perp}$  and is comparable to  $\eta_{\text{eff}}$  measured in the rheometer. Just below the  $N-I$  transition the director is aligned along the flow direction and  $\eta_{\parallel}$  is nearly equal to the Miesowicz viscosity, i.e.,  $\eta_{\parallel} \cong \eta_2 = (\alpha_3 + \alpha_4 + \alpha_6)/2$ . In the nematic phase  $\eta_{\parallel} < \eta_{\perp}$  ( $\cong \eta_3 = \alpha_4/2$ ) and both increase as the temperature is reduced;  $\eta_{\text{eff}}$  also increases with temperature, but the relative rate of increase of the former two is larger. Two considerations can be made to understand their temperature dependence. First, apart from the temperature effect, the viscosity can also increase as the smectic phase is approached due to the occurrence of temporary smectic clusters in the bulk. Second, the colloids are coated with DMOAP, which promotes homeotropic alignment of the bent-core molecules. On the surface of the microsphere the free rotation of the molecules along the long axis is restricted due to steric hindrance; as a result they are pinned in a facilitating formation of *permanent* smectic clusters or layers around the microspheres. As a result, the hydrodynamic radius of the microsphere could be significantly larger than the actual radius due to the large cloud of the distorted nematic around the microsphere. Assuming  $\eta_{\parallel} = \eta_{\text{eff}} = 21.6 \text{ mPa s}$  near the  $N-I$  transition ( $T - T_{N-I} = -18^\circ\text{C}$ ), the estimated hydrodynamic radius of the microsphere is  $0.68 \mu\text{m}$ , which is about  $0.2 \mu\text{m}$  larger than the actual radius. A schematic molecular orientation of bent-core molecules and some clusters around the microsphere with a dipolar defect is shown in Fig. 6. In fact, it was shown that both diffusion coefficients ( $D_{\parallel}$  and  $D_{\perp} \propto 1/\eta$ ) decreases when the size of the microsphere is greater than  $0.5 \mu\text{m}$ , which is attributed to the effective size of the microsphere, which is much bigger than the geometric size [20]. In addition, the smectic layering effect can increase with decreasing temperature due to a kind of condensation of the clusters around the microsphere effectively increasing



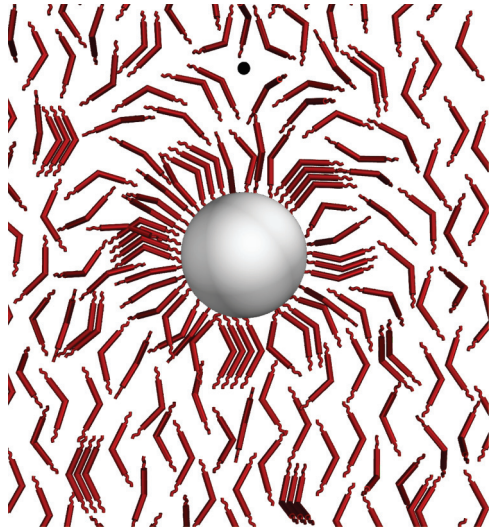


FIG. 6. (Color online) Schematic molecular orientation around the microsphere with a dipolar defect configuration. It may be noted that the clusters attached to the microsphere are permanent, whereas they are temporal in nature in the bulk. The small dot near the top indicates a hyperbolic hedgehog.

the diameter of the microsphere with decreasing temperature. As the temperature is further reduced and we approach the Sm-C phase, interestingly we notice that  $\eta_{||}$  tends to diverge around 24 °C above the N-Sm-C transition. To understand this we look at the Brownian trajectory of a microsphere. The two-dimensional projection of the trajectories of a microsphere near N-I ( $T - T_{N-I} = -7.6$  °C) and N-Sm-C ( $T - T_{N-I} = -47.6$  °C) transitions are shown in the inset of Fig. 5. We notice that the fluctuations are highly restricted near the N-Sm-C transition compared to the N-I transition. Since the cell is rubbed, it is expected that the smectic layer planes in the temporarily fluctuating clusters are oriented perpendicular to the rubbing direction. In this case the fluctuating clusters are large enough and the self-diffusion of the microparticle in the direction perpendicular to the layer plane is expected to be lower than that in parallel direction and as a result  $\eta_{||}$  can diverge.

Finally, we would like to comment on the Brownian fluctuations near and far from the N-Sm-C transitions for longer time intervals (3 s). In Fig. 7 we show the histograms of the Brownian fluctuations of the microsphere parallel and perpendicular to the director at a time interval  $\tau = 3$  s. The perpendicular component appears to fit reasonably well with

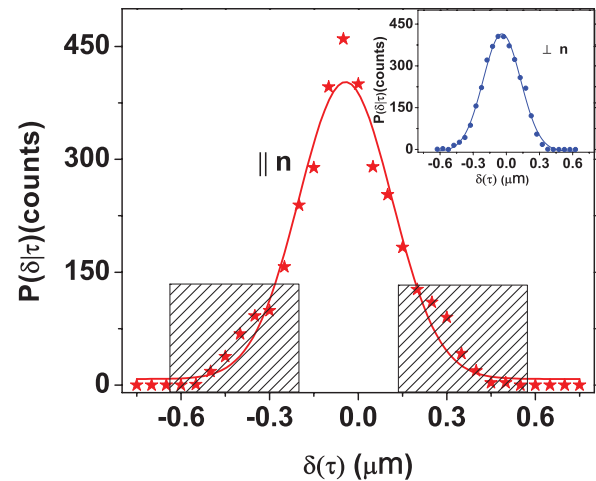


FIG. 7. (Color online) (a) Histograms of particle displacement parallel ( $||$ ) and perpendicular ( $\perp$ ) to the director for  $\tau = 3$  s. The solid lines are Gaussian fits to the data. The tail parts that significantly deviate from the fittings are highlighted by shaded regions.

the Gaussian distributions (Fig. 7). In the case of the parallel component the distribution is complex in the sense that it cannot simply be fitted to a Gaussian function. Similar non-Gaussian distributions are observed in many physical systems [30]. In the case of soft materials the diffusion of unilamellar lipid vesicles (liposomes) in solutions of aligned F-actin filaments was reported recently by Wang *et al.* [30]. It was shown that this behavior is mainly due to the slowly varying heterogeneous fluctuations in the environment. In their experiment it was reported that the distribution in the perpendicular direction shows exponential tails, whereas in the parallel direction the central and tail parts can be fitted with two Gaussian functions with different widths. In our present experiment the perpendicular components appear to be Gaussian, whereas the parallel component deviates significantly. Based on the same argument, we anticipate that even in our case, the non-Gaussian fluctuations of the parallel component are due to the slow fluctuations of the temporarily smectic clusters whose layer normal is parallel to the rubbing direction. This, however, needs to be substantiated by more experiments as well as simulations.

We gratefully acknowledge the support from the DST (Grant No. SR/NM/NS-134/2010) and CSIR (Grant No. 03(1207)/12/EMR-II and PURSE, UOH). Y.B. acknowledges ACRHEM for financial support.

- [1] P. G. de Gennes, *The Physics of Liquid Crystals*, 2nd ed. (Oxford University Press, Oxford, 1993).
- [2] S. Chandrasekhar, *Liquid Crystals*, 2nd ed. (Cambridge University Press, Cambridge, 1992).
- [3] V. V. Belyaev, *Viscosity of Nematic Liquid Crystals*, 1st ed. (Cambridge International Science, Cambridge, 2011).
- [4] F. M. Leslie, *J. Mech. Appl. Math.* **19**, 357 (1966).

- [5] T. Carlsson and K. Skarp, *Mol. Cryst. Liq. Cryst.* **104**, 307 (1984).
- [6] C. R. Safinya, E. B. Sirota, and R. J. Plano, *Phys. Rev. Lett.* **66**, 1986 (1991).
- [7] K. Negita, M. Inoue, and S. Kondo, *Phys. Rev. E* **74**, 051708 (2006).
- [8] J. Ananthaiah, M. Rajeswari, V. S. S. Sastry, R. Dabrowski, and S. Dhara, *Eur. Phys. J. E* **34**, 74 (2011).

- [9] H. Takezoe and Y. Takanishi, *Jpn. J. Appl. Phys.* **45**, 597 (2006).
- [10] R. A. Reddy and C. Tschierske, *J. Mater. Chem.* **16**, 907 (2006).
- [11] D. B. Wiant, J. T. Gleeson, N. Eber, K. Fodor-Csorba, A. Jakli, and T. Toth-Katona, *Phys. Rev. E* **72**, 041712 (2005).
- [12] D. Wiant, S. Stojadinovic, K. Neupane, S. Sharma, K. Fodor-Csorba, A. Jakli, J. T. Gleeson, and S. Sprunt, *Phys. Rev. E* **73**, 030703 (2006).
- [13] V. Domenici, C. A. Veracini, and B. Zalar, *Soft Matter* **1**, 408 (2005).
- [14] B. R. Acharya, A. Primak, and S. Kumar, *Phys. Rev. Lett.* **92**, 145506 (2004).
- [15] L. A. Madsen, T. J. Dingemans, M. Nakata, and E. T. Samulski, *Phys. Rev. Lett.* **92**, 145505 (2004).
- [16] J. Harden, B. Mbanga, N. Éber, K. Fodor-Csorba, S. Sprunt, J. T. Gleeson, and A. Jakli, *Phys. Rev. Lett.* **97**, 157802 (2006).
- [17] S. Stojadinovic, A. Adorjan, S. Sprunt, H. Sawade, and A. Jakli, *Phys. Rev. E* **66**, 060701 (2002).
- [18] P. Sathyanarayana, M. Mathew, Q. Li, V. S. S. Sastry, B. Kundu, K. V. Le, H. Takezoe, and S. Dhara, *Phys. Rev. E* **81**, 010702(R) (2010).
- [19] S. Dhara, F. Araoka, M. Lee, K. V. Le, L. Guo, B. K. Sadashiva, K. Song, K. Ishikawa, and H. Takezoe, *Phys. Rev. E* **78**, 050701(R) (2008).
- [20] M. Skarabot and I. Musevic, *Soft Matter* **6**, 5476 (2010).
- [21] J. Ananthaiah, M. Rajeswari, V. S. S. Sastry, R. Dabrowski, and S. Dhara, *Phys. Rev. E* **86**, 011710 (2012).
- [22] C. Bailey, K. Fodor-Csorba, J. T. Gleeson, S. N. Sprunt, and A. Jakli, *Soft Matter* **5**, 3618 (2009).
- [23] K. Negita and H. Kaneko, *Phys. Rev. E* **80**, 011705 (2009).
- [24] V. Prasad, S. W. Kang, K. A. Suresh, L. Joshi, Q. Wang, and S. Kumar, *J. Am. Chem. Soc.* **127**, 17224 (2005).
- [25] H. G. Yoon, S. W. Kang, R. Y. Dong, A. Marini, K. A. Suresh, M. Srinivasarao, and S. Kumar, *Phys. Rev. E* **81**, 051706 (2010).
- [26] K. Van Le, M. Mathews, M. Chambers, J. Harden, Q. Li, H. Takezoe, and A. Jakli, *Phys. Rev. E* **79**, 030701(R) (2009).
- [27] B. Senyuk, H. Wonderly, M. Mathews, Q. Li, S. V. Shiyonovskii, and O. D. Lavrentovich, *Phys. Rev. E* **82**, 041711 (2010).
- [28] P. Sathyanarayana, T. Arun Kumar, V. S. S. Sastry, M. Mathews, Q. Li, H. Takezoe, and Surajit Dhara, *Appl. Phys. Express* **3**, 091702 (2010).
- [29] J. C. Loudet, *Liq. Cryst. Today* **14**, 1 (2005).
- [30] B. Wang, J. Kuo, S. C. Bae, and S. Granick, *Nat. Mater.* **11**, 481 (2012), and references therein.